Optics Letters

High-power Yb-based all-fiber laser delivering 300 fs pulses for high-speed ablation-cooled material removal

Parviz Elahi,[1] Önder Akçaalan,[1] Cansu Ertek,[2] Koray Eken,[2]
F. Ömer Ilday,[1,3,4] and Hamit Kalaycıoğlu[1,*]

[1]Department of Physics, Bilkent University, Ankara 06800, Turkey
[2]FiberLAST, A.S., Ankara 06531, Turkey
[3]Department of Electrical and Electronics Engineering, Bilkent University, Ankara 06800, Turkey
[4]UNAM–National Nanotechnology Research Center and Institute of Materials Science and Nanotechnology, Bilkent University, Ankara, 06800, Turkey
*Corresponding author: hamitkal@bilkent.edu.tr

We report on a 72 W Yb all-fiber ultrafast laser system with 1.6 GHz intra-burst and 200 kHz burst repetition rate developed to demonstrate ablation-cooled material removal at high speeds. Up to 24 W is applied on Cu and Si samples with pulses of ~300 fs, and record-high ablation efficiencies are obtained, compared to published results to date, despite using only ~100 nJ pulses. Ablation speeds approaching 1 mm^3/s are reported with 24 W of average power, limited by available laser power and beam scanning speed. More significantly, these results experimentally confirm the theoretically expected linear scaling of the ablation-cooled regime to higher average powers without sacrificing efficiency, which implies that further scaling is possible with further increases in laser power and scanning speeds.   © 2018 Optical Society of America

Material processing with ultrafast pulses has superb aspects as minimal collateral damage and high precision with the downsides of traditionally being a slow process, requiring complex high-energy lasers [1]. The recently demonstrated ablation-cooled laser material regime [2] opened the door to transcending the limited ablation rates and the need for tens to hundreds of microjoules. In this regime, the repetition rate has to be high enough that there is insufficient time for the targeted spot size to cool down substantially by heat conduction into the rest (bulk) of the target material by the time the next pulse arrives. Subsequent pulses ablate a target material that is already extremely hot, thereby reducing the individual pulse energy threshold. For example reduction of three orders of magnitude for Cu [2] was obtained compared to published results. While the results supported the claims we proposed for the new regime, they were obtained with Watt-level powers. It would be very interesting for industrial applications to scale the power up and investigate this regime for potential use in mass production.

The ablation-cooled material removal regime is particularly advantageous for fiber lasers, which have major practical advantages such as excellent beam quality, low cost, high average power, and high robustness, but are severely limited in pulse energy compared to solid state lasers. Despite the reduction of the required pulse energy (typically fractions of a microjoule), the need for high repetition rates (typically in the GHz range) can only be met through burst-mode operation, where groups of high-repetition pulses are repeated at a much lower frequency. By controlling the time between the bursts, i.e., the burst repetition rate, the average power can be kept at reasonable levels. As a matter of fact, the burst mode was first demonstrated as a powerful tool for material processing in 1999 [3]. With this perspective, we embarked on the development of ultrafast burst-mode fiber lasers and demonstrated the first such laser [4]. This was followed by the development of control electronics for uniform intra-burst pulse energy distribution [5], scaling the burst repetition rates to 1 MHz and 100 W [6], investigating the limits of pulse-pumped and continuously pumped burst-mode laser systems by characterizing amplified spontaneous emission (ASE) and achieving 40 μJ pulses in the pulse-pumped regime and 145 W average power in the continuously pumped systems [7,8]. All of these employed a 100 MHz seed laser, and more recently we developed a laser amplifier with an adjustable intra-burst repetition rate up to 3.5 GHz [9]. In the meantime, Breitkopf *et al.* demonstrated an impressively high-energy (58 mJ) rod-fiber burst-mode amplifier [10], opening up new possibilities.

Here, we present a Yb-based all-fiber burst-mode laser amplifier built to demonstrate ablation-cooled material removal in

the high-power range. This is a 1.6 GHz intra-burst system able to produce a 72 W (30 W) amplifier output at a 200 kHz burst repetition rate before (after) dechirping in an external grating compressor. The dechirped pulse duration is around 300 fs. The dechirped burst energy is 155 µJ. The number of pulses in the burst is electronically adjustable. For 800 pulses per burst (burst duration of 500 ns), an individual pulse energy is ~0.19 µJ. The laser was tested in ablation experiments on Cu and Si samples where up to 24 W could be applied on the samples. The ablation efficiency and pulse energy scaling results confirm that the ablation cooling regime is scalable to higher average powers with a linear increase in processing speed.

The Yb-fiber laser system (Fig. 1) consists of an all-fiber dispersion-managed oscillator, followed by three stages of amplification and a fiber-coupled acousto-optic modulator (AOM) located after the first amplifier, which imposes the burst pattern on the pulse train. The 100 MHz oscillator with an overall positive cavity dispersion of 3450 fs^2 generates a seed signal of 18 mW via the coupler port of a hybrid WDM. The seed spectrum width [Fig. 2(a)] and pulse duration [Fig. 2(b)] are measured to be 19 nm and ~2 ps, respectively, after the signal traverses 60 cm of a single-mode (SM) fiber (HI1060) at the output of the coupler. Following the oscillator, the seed pulses are stretched to 44 ps with 57 m of SM fiber and fed to a repetition rate multiplier made up of five 3 dB fiber optic couplers, which increases the repetition rate by a factor of 2^4 to 1.6 GHz [Fig. 2(c)] [9]. Due to losses of couplers, the signal

power drops down to ~5 mW, which is increased to 112 mW by a SM preamplifier made of a highly doped gain fiber (20 cm Yb 125 by CorActive). The spectrum is measured after the pre-amplifier to have a width of 15 nm [Fig. 2(d)]. At the output of the AOM (55% insertion loss), the power drops to 5 mW for 800-pulse bursts repeated at 200 kHz with a duty cycle of 10%. Next, the 5 mW signal is amplified to 150 mW via a two-stage SM amplifier, where 330 mW pump power is distributed to two gain fiber segments (40 cm of Yb 64, 22 cm of Yb 125) by a 20/80 coupler, respectively.

At the final section of the laser system, the power amplifier consists of four 25 W multimode diodes and 4 m of 30 µm core diameter double-clad (DC) gain fiber (30/125 Yb1200 by nLight). The signal is boosted from 150 mW to 72 W with a pump power of 92 W for, yielding a notable pump to signal conversion efficiency of 78%. For 800-pulse bursts at 200 kHz, this means an amplified burst energy of 360 µJ, and individual pulse energy of ~450 nJ. A fiber coupled collimator-isolator at the output of the amplifier protects the system especially in material processing experiments. The pulse train, radio frequency (RF) spectrum, and optical spectrum of the output is shown in Fig. 2(e)–2(g), respectively. Fairly uniform energy distribution inside the burst [Fig. 2(e)] is a consequence of the continuous pumping, which minimizes the gain depletion. The main lobe in the RF spectrum [Fig. 2(f)] centered at 1.6 GHz with a 3 dB width of 2 MHz indicates the intra-burst repetition rate and 500 ns duration of the 800-pulse bursts, while the
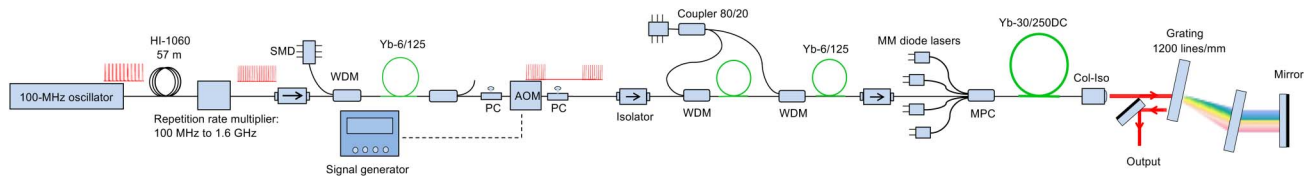
Fig. 1. Schematic diagram of the laser system. SMD, single-mode diode; WDM, wavelength division multiplexer; MM, multimode; Col-Iso, collimator-isolator; MPC, multimode pump-signal combiner; DC, double-clad; AOM, acousto-optic modulator; PC, polarization controller.
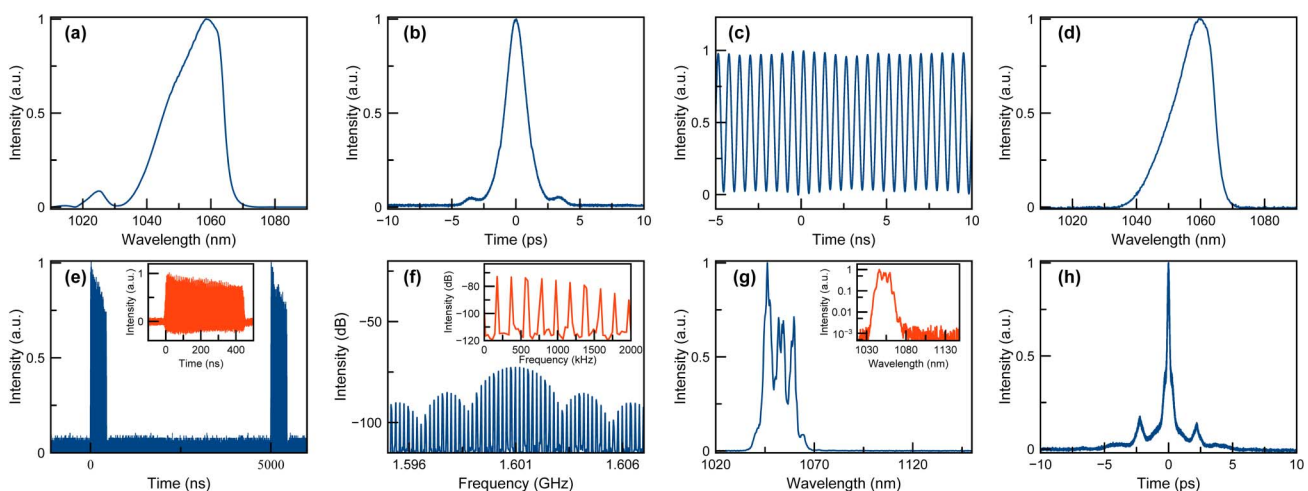

Fig. 2. Oscillator characterization. (a) The optical spectrum from output port measured after 60 cm SM fiber, (b) the intensity autocorrelation of the pulses measured at the same location as the spectrum in (a). (c) 1.6 GHz pulse train at the output of the repetition rate multiplier. (d) Optical spectrum at output of first preamplifier. Amplifier characterization for 500-ns (800-pulse) long bursts at 72 W. (e) Measured pulse train (inset: single burst), (f) the RF spectrum of the amplified burst train with 12 MHz span and 1 kHz resolution (inset: close-up with 2 MHz span and 1 kHz resolution showing the comb lines corresponding to the burst repetition frequency of 200 kHz), (g) optical spectrum of the amplified output (inset: semi-log version), (h) measured autocorrelation of the compressed pulses of 450 nJ individual energy.

closeup in the inset demonstrates the 200 kHz burst repetition rate. The pulses are compressed with a pair of 1200 line/mm transmission gratings down to the 270 fs level, as inferred from the autocorrelation measurement results [Fig. 2(h)] assuming a Gaussian pulse shape. The throughput efficiency of the polarization-sensitive compressor is a mere 43% due to the unpolarized nature of the amplifier output. The combined loss of the collimator-isolator and compressor reduces the power down to 28 W and with a further cut at the input aperture of the galvo scanner (Scancube14 by Scanlab), the maximum power available for material processing is 24 W.

The material processing performance of the high-power laser system was tested on samples of Cu and Si, which are important technological materials. The ablation efficiency was investigated by measuring the volume of spots ablated by single bursts with no overlap between consecutive bursts, repeated at 200 kHz. Three different cases of bursts, containing 720, 560, and 400 pulses, with power levels in each case corresponding to individual pulse energies of 83, 110, 138, and 167 nJ with highest level of 24 W (720-pulse burst, 166 nJ pulse energy) were applied to samples. The spot size formed by the $f =$ 5.6 cm f-theta lens of the galvo scanner was measured with a beam profiler to be 23 μm ($1/e^2$ diameter) with an ellipticity of 0.98, indicating the high axial symmetry of the focal spot. The ablation volume was measured with a laser scanning microscope (LSM-Keyence VK-100x) by taking the average of several spots for each energy level while the corresponding fluence was calculated in terms of the incident burst energy per area of the laser spot. The ablated volume results versus the incident

fluence are shown in Figs. 3(a) and 3(b), for Cu and Si, respectively, together with relevant data from our previous work [2]. Here, the incident fluence instead of the burst energy is used as the variable parameter specifically to account for the difference in the spot sizes between the current system (23 μm) and that used in [2] (26 μm). Also, the material removal efficiency (MRE) (ablated volume per burst × 200 kHz × 60 s/ min / incident average power) for each result in Figs. 3(a) and 3(b) versus the incident pulse energy is plotted in the insets of Figs. 3(a) and 3(b), for Cu and Si, respectively. Examples of the scanning electron microscope (SEM) views and the LSM depth profiles of the ablation holes on the Cu and Si samples are given in Figs. 3(c)–3(f).

The efficiency results [Fig. 3(a)] for Cu support the pulse energy scaling principle of the ablation cooling regime as they locate in the same range with the data of the 800-pulse and 400- pulse bursts with intra-burst repetition rates of ~3.5 and 1.7 GHz, respectively, from our previous work [2]. As a matter of fact, for Cu the fluence of ~10 J/cm² realized with 560-pulse bursts per spot indicates an individual pulse fluence of ~0.02 J/cm², which is at least 10 times lower than the threshold fluence data reported in the literature (0.23–0.3 J/cm²) [11–13]. The maximum volume (500 μm³) on Cu is obtained with a single burst containing 560 pulses and 93 μJ burst energy (167 nJ average pulse energy) at a fluence of 22.4 J/cm². The material removal rate is calculated as 500 μm³ × 200 kHz = 6 mm³/ min. On the other hand, the removal efficiency for Cu [inset of Fig. 3(a)] peaks at 0.39 mm³/ min /W for 400-pulse bursts with individual pulses of merely 110 nJ (44.5 μJ
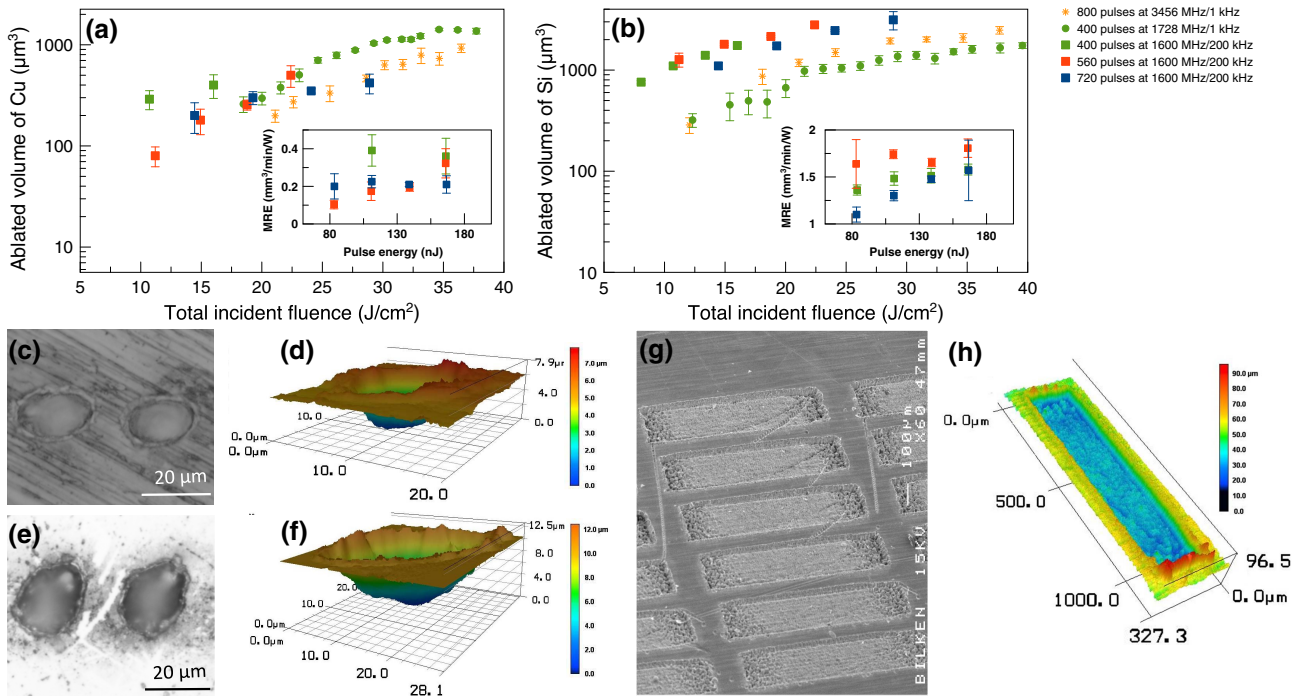
Fig. 3. Overview of the material processing performance of the high-power laser system. The ablated volume versus the incident fluence on the (a) Cu and (b) Si samples with one burst incident per spot. The results with a 1 kHz burst repetition rate from previous work [2] are also included for comparison. Inset to (a) and (b): the material removal efficiency (MRE) versus incident pulse energy for the Cu and Si samples, respectively, for the high-power laser. Examples of scanning electron microscope (SEM) views of ablation spots on (c) Cu and (e) Si, and examples of depth profiles of the ablation holes obtained with the LSM on (d) Cu and (f) Si. (g) the SEM view of trenches ablated by 4-pass raster scans on Cu and (h) the LSM view of a sample trench.

burst energy, 10.7 J/cm^2 fluence, 8.9 W average power) which generate an ablation of 290 μm^3 per burst. Reviewing the highest performances in ultrafast processing of Cu published to date, Schille *et al.* have reported 6.3 mm^3/ min and 0.2 mm^3/ min /W with sub-ps pulses at 6.4 MHz and 31 W applied power (4.9 μJ pulse energy) [12], and Neuenschwander *et al.* reported 0.13 mm^3/ min /W with sub-ps pulses at 200 kHz and 4 W applied (20 μJ pulse energy) [13]. Hence, two-fold improvement in material removal efficiency is achieved relative to the best previous result, while the individual pulse energy is remarkably reduced by 44 times (110 nJ versus 4.9 μJ).

In case of Si, the high-power system produced two to three times higher ablation per spot [Fig. 3(b)] relative to the similar modes of the low-power system (bursts at 1 kHz with 400-pulse, 1.7 GHz intra-burst and 800-pulse, 3.5 GHz intra-burst). Pulse scaling is evident with a threshold fluence below 8 J/cm^2, indicating a threshold below 0.02 J/cm^2 per pulse for 400-pulse bursts, which is at least ten times below the fluence levels reported in the literature (∼0.2 J/cm^2 [14,15]). The ablated volume with one burst reaches a maximum value of 3100 μm^3 for 720-pulse bursts and 24 W average power (120 μJ burst energy). Converting to the material removal rate in the same manner as Cu above, we obtain 37.2 mm^3/ min. For Si, the highest removal efficiency [inset of Fig. 3(b)] of 1.8 mm^3/ min /W occurs for 560-pulse bursts with 167 nj pulses (93.3 μJ burst energy, 22.4 J/cm^2, 18.7 W). Compared with the best performances for Si processing to date with 1 μm ultrafast lasers, this is more than two times better in the material removal rate and 3 times better in the removal efficiency than 15 mm^3/ min and 0.5 mm^3/ min /W, respectively, obtained by 6-pulse bursts containing 8 μJ pulses and a 1 MHz burst repetition rate in Ref. [16]. However, the most striking aspect of this comparison is that the pulse energy for our laser at the highest level of removal efficiency is 48 times lower than that of the comparison (167 nJ versus 8 μJ). We also note that, even at 100 nJ per pulse, the ablation efficiency is still very impressive [inset of Fig. 3(b)]. On the other hand, the superior performance of this system on Si relative to the low-power one [Fig. 3(b)] may have implications of high-power effects that deserve further investigation and will be the subject of our future studies.

As an independent confirmation of the accuracy of our method of measurement based on laser scanning microscopy, volume ablation experiments were done with Cu samples, where LSM measurements were compared with weight-loss measurements. First, raster scanning the laser beam over a rectangular area of 1 mm by 200 μm with 720-pulse bursts at 200 kHz and 24 W on the sample, three ablation trenches were formed scanning the laser over the target area twice, three times, and four times. Using the LSM, the volume of the trenches was measured to be 1, 2.1, and 3.8 × 10^6 μm^3 for the two, three, and four pass scans, respectively. These results yielded an average ablated volume of 0.77 × 10^6 μm^3 for one pass. Second, weight-loss measurements were done where the weight of three samples were measured with a high-precision scale of 0.10 mg sensitivity before and after processing. A total of 96 four-pass raster scans were performed with the same parameters as the first case. The total weight of the three samples was measured to be 1346.5 and 1343.7 mg before and after, respectively. A difference of 2.8 mg indicated 29.2 μg of weight loss per a four-pass scan and therefore 7.3 μg per single-pass ablation. This is converted to a volume of 0.814 × 10^6 μm^3 using the Cu density (8.96 g/cm^3). Hence,

the accuracy of the LSM measurements was firmly established. The SEM view of a section of the trenches generated by 4-pass raster scans for the weight-loss measurements is shown in Fig. 3(g) and the LSM profile of one of those trenches is given in Fig. 3(h).

In conclusion, we have demonstrated a 72 W femtosecond-pulsed laser system built for ablation-cooled material processing. This is the highest power reported for a burst-mode fiber laser generating femtosecond pulses, to the best of our knowledge. Using this system, we have shown that the material processing results reported, mainly at 1 kHz in Ref. [2], scale favorably to 200 kHz with no evidence of reduction in efficiency. We obtained ablation threshold fluence (per pulse) of ∼0.02 J/cm^2 for both Cu and Si, which is at least ten times below the reported values for both materials. The maximum material removal efficiencies of 0.39 mm^3/ min /W and 1.8 mm^3/ min /W obtained with pulse energies of 110 nJ and 167 nJ for Cu and Si, respectively, surpass the data in the literature to date (0.2 and 0.5 mm^3/ min /W for Cu and Si, respectively) while reducing the pulse energy by nearly 50 fold. While the observed scaling was theoretically expected, its experimental confirmation is important as it points the way forward as higher laser powers become available. Considering that merely ∼100 nJ of pulse energies were shown to be sufficient for ablation with record-high efficiencies, our results suggest exciting prospects for fiber laser technology in architectures and fiber types for which all their practical advantages remain intact, being applied to industrial laser-material processing, a domain hitherto served primarily by high-energy solid state or hybrid lasers.

REFERENCES

1. K. Sugioka and Y. Cheng, Light Sci. Appl. **3**, e149 (2014).
2. C. Kerse, H. Kalaycıoğlu, P. Elahi, B. Çetin, D. K. Kesim, Ö. Akçaalan, S. Yavaş, M. D. Aşık, B. Öktem, H. Hoogland, R. Holzwarth, and F. Ö. Ilday, Nature **537**, 84 (2016).
3. M. Lapczyna, K. Chen, P. Herman, H. Tan, and R. Marjoribanks, Appl. Phys. A **69**, S883 (1999).
4. H. Kalaycioglu, K. Eken, and F. Ö. Ilday, Opt. Lett. **36**, 3383 (2011).
5. H. Kalaycıoğlu, Y. Eldeniz, Ö. Akçaalan, S. Yavaş, K. Gürel, M. Efe, and F. Ö. Ilday, Opt. Lett. **37**, 2586 (2012).
6. P. Elahi, S. Yılmaz, Y. Eldeniz, and F. Ilday, Opt. Lett. **39**, 236 (2014).
7. H. Kalaycıoğlu, Ö. Akçaalan, S. Yavaş, Y. Eldeniz, and F. Ö. Ilday, J. Opt. Soc. Am. B **32**, 900 (2015).
8. S. Yılmaz, P. Elahi, H. Kalaycıoğlu, and F. Ö. Ilday, J. Opt. Soc. Am. B **32**, 2462 (2015).
9. C. Kerse, H. Kalaycıoğlu, P. Elahi, Ö. Akçaalan, and F. Ö. Ilday, Opt. Commun. **366**, 404 (2016).
10. S. Breitkopf, A. Klenke, T. Gottschall, H.-J. Otto, C. Jauregui, J. Limpert, and A. Tunnermann, Opt. Lett. **37**, 5169 (2012).
11. G. Raciukaitis, M. Brikas, P. Gecys, B. Voisiat, and M. Gedvilas, J. Laser Micro. Nanoeng. **4**, 186 (2009).
12. J. Schille, L. Schneider, P. Lickschat, U. Loeschner, R. Ebert, and H. Exner, J. Laser Appl. **27**, S28007 (2015).
13. B. Neuenschwander, B. Jaeggi, M. Zimmermannn, V. Markovic, B. Resan, K. Weingarten, R. de Loor, and L. Penning, J. Laser Appl. **28**, 022506 (2016).
14. J. Bonse, S. Baudach, J. Krüger, W. Kautek, and M. Lenzner, Appl. Phys. A **74**, 19 (2002).
15. J. Thorstensen and S. Erik Foss, J. Appl. Phys. **112**, 103514 (2012).
16. R. Knappe, H. Haloui, A. Seifert, A. Weis, and A. Nebel, Proc. SPIE **7585**, 75850H (2010).